SSRG International Journal of Electrical and Electronics Engineering
ISSN: 2348-8379/ https://doi.org/10.14445/23488379/IJEEE-V12I4P111

Volume 12 Issue 4, 155-169, April 2025
© 2025 Seventh Sense Research Group®

Original Article

Firefly Optimized Controllers for Frequency Stabilization in an Interconnected Micro-Grid Fed with Solar PV Systems and Electric Vehicles

Endoori Rani[1], K. Naga Sujatha[2]

[1,2]*EEE Department, JNTUH UCEST, JNTUH University, Telangana, India.*

[1]*Corresponding Author : priyaraniendoori987@gmail.com*

Received: 08 February 2025 Revised: 10 March 2025 Accepted: 11 April 2025 Published: 29 April 2025

Abstract *- Microgrids (MGs) rely heavily on Renewable Energy Sources (RES), making frequency stability a top need. The indeterminate load patterns and inconsistent behaviour of energy from natural sources worsen this issue. This manuscript tackles the concern of regulating frequency in a two-area MG system incorporating an equal number of diverse energy sources like Photovoltaic (PV) systems, aqua-electrolyzers, turbines for wind, devices for energy storage, Automobiles with Electric Power, Bio-gas generators and fuel cells in Area 1 as well as Area 2. Addressing the challenge of Load Frequency Management (LFM), classical controllers, including I, PI, and PID, which stand for integral, proportional, and derivative, respectively, are employed and enhanced by applying the Firefly Algorithm (FA). Simulation results reveal the PID controller's superior performance, characterized by minimal settling periods and peak amplitude deviations. Moreover, the FA-PID controller tuned with the FA technique exhibits robust performance under varying demand conditions and demonstrates insensitivity to significant deviations in load demands.*

Keywords *- Electric vehicle, Frequency deviation, Interconnected two-area micro grid, Renewable Energy Sources, Solar PV system.*

1. Introduction

Reliable electricity generation is the backbone of modern society, powering industries and driving economic growth. Power-generating systems must deliver a consistent and stable electricity supply to meet the demands of an increasingly complex and interconnected world. A significant electrical system is designed to be resistant to disturbances, agile in reaction to changes in energy consumption, and adaptive to shifting load needs. However, when uncertainty hits, the impacts can be severe enough, resulting in the shedding of loads and, in worst-case scenarios, extensive power blackouts. Furthermore, the inherent variability of demand for power offers a substantial issue. Variations in load needs immediately affect system electrical frequency and inter-grid power transmission, resulting in departures from ideal operating conditions [1]. The demand for higher versatility, increased dependability, a smaller ecological impact, and the easy incorporation of variable sources of clean energy is driving the transition to microgrids. Microgrids provide an innovative method for conserving energy, using regional renewable energy sources to reduce dependency on consolidated power networks while fostering more resilient and environmentally friendly energy systems. Microgrid operation requires balancing power generation with load requirements while considering transmission losses [2]. Frequency variations and tie-line power transfers might happen while microgrid systems expand, posing a risk to equipment and jeopardizing system reliability. Electricity systems confront underlying unpredictability and uncertainty owing to varying load demands. This influences frequency variation and power transfer within linked grids, producing departures from their typical operating norms [3]. Integrating clean energy sources into microgrids and linked microgrids has attracted a lot of interest due to its ability to cut carbon emissions and improve dependability. However, because these systems have a smaller capacity, they have less inertia. They are more subject to fluctuating frequencies produced by random RES output and probabilistic demands for load. Effective control mechanisms are required to overcome this difficulty, notably secondary control of frequencies or management of load frequency. Maintaining the system's frequency and tying the power exchange together requires LFM within proper constraints. However, integrating many interrelated components adds complexities to LFM, which demands establishing strong control techniques and optimum algorithms to ensure effective functioning [4-7]. The difficulty of Load Frequency Management (LFM) increases when coordinating numerous linked components [8, 9]. Modern electrical systems require complex control techniques and finely tuned-algorithmic optimization to function optimally. Developing intricate control strategies backed by well-designed algorithms is necessary to guarantee the best possible electrical network performance. Researchers have investigated a number of computational techniques for reducing frequency deviations and enhancing Automatic Generation Control (AGC) with the purpose of improving the Load Frequency performance Management (LFM) management system. These regulators' principal job is to modify subsystems' electrical output during unbalanced circumstances, which is accomplished by making precise changes to diesel/biodiesel generator valve settings and strategically manipulating extra power components.

The most important parameter for these actuators is the (μACE/ ACE) Micro-area or Area Control Error [10, 11]. Even when load demand varies, Load Frequency Controls (LFC) make maintaining the system's frequency steady within predetermined bounds simpler. LFC, a critical component of power system stability under different load conditions, provides a balanced power exchange across linked areas [12]. The frequency is disrupted and deviates beyond allowable bounds when the generator's power output is insufficient to meet the system's overall demand. Frequency stability is a major issue associated with modern electrical systems, especially in microgrids, where electric cars and renewable energy sources are widely used [13]. Integrating solar Photovoltaic (PV) systems and Electric Vehicles (EVs) introduces additional difficulties in preserving frequency stability due to their sporadic and variable nature. PID controllers are the cornerstone of conventional frequency regulating methods and have been extensively used in power systems due to their effectiveness and simplicity [14].

Autonomous systems for control, including protection relays that switch off generators from the power grid or initiate load shedding, are activated to regain the normal frequency. Reliable electrical system functioning requires lowering settling time and frequency fluctuations (undershoots and overshoots). Adding extra controllers will help achieve this objective [15]. Advanced techniques for optimization are used to precisely adjust controller performance and enhance the system's capacity to lower frequency fluctuations and maintain rigidity. Conventional approaches for studying autonomous generating control within networked power systems have used regulators like an integral, PI, PID, and Dual Integration Differentiation [16, 17]. The intricate dynamics of contemporary microgrids, which heavily rely on renewable energy sources and electric vehicles, maybe too much for PID controllers to manage. Nevertheless, the efficiency of these actuators is frequently reduced by the many scenarios of operation seen in these systems. Sliding-mode controls [18, 19], fuzzy reasoning algorithms [20, 21], proportional matrix inequity control [22, 23], predicting and adaptable control [24, 25], the best control approach [26, 27], and model-based predictive control [28, 29] are some of the sophisticated management methodologies that have arisen in response. The availability of sophisticated electronic instruments has influenced the advancement of regulation approaches, allowing for the expansion of creative controllers that make Flexible AC Transmission Systems (FACTS) [30, 31], along with other use of solutions for storing energy [32, 33], revolutionary technologies. FACTS controllers greatly increase energy transfer capacity and overall network integrity by controlling the flow of electricity across linked lines of communication [34, 35]. The advancement of sophisticated soft computing methods is underway to improve actuator reliability [36, 37].

PID controller settings for frequency stabilization in micro-grids have been optimized in recent years using techniques for optimization, including Genetic Algorithms (GA), Particle Swarm Optimization (PSO), and Ant Colony Optimization (ACO) [38-40]. These optimization methods do, however, have drawbacks, including problems with convergence and computing complexity [41]. Artificial bee colony algorithms, bacterial foraging methods [42, 43], bat-inspired algorithms [44, 45], cuckoo search optimization [46-48], differential evolution algorithms [49, 50], and genetic PSO approaches [51, 52] are just a few examples of the various soft computing approaches. Firefly algorithms [57, 58], learning and instruction-oriented optimization [55, 56], and quasi-oppositional harmony search strategies [53, 54] have all been developed to handle the complexity of nonlinear connected power systems. The relatively new optimization technique called the Firefly Optimization Algorithm (FOA) was inspired by the flashing behaviour of fireflies. Complex optimization issues, such as those in power systems, have been demonstrated to be successfully resolved using FOA [59].

Nevertheless, not much research has been done on using FOA to improve PID controller settings for frequency stability in microgrids, including EVs and solar PV systems. Maintaining frequency stability becomes more difficult when solar photovoltaics and electric cars are integrated into the power system. Frequency discrepancies are caused by varying EV charging and discharging patterns and intermittent solar production. To lessen these effects, sophisticated techniques are required as traditional management approaches are inadequate. For contemporary microgrids, traditional PID controllers might not be enough. The majority of current research on micro-grid frequency stabilization uses optimization methods, including particle swarm optimization and evolutionary algorithms, as well as conventional PID controllers. These techniques struggle to handle the complicated dynamics of modern microgrids, especially those with significant integration of renewable energy sources and electric cars. A new firefly-optimized control method for frequency stabilization is presented in this research. The strategy optimizes controller settings using the Firefly algorithm. This makes stability improvement and efficient frequency control possible. The complexity of contemporary micro-grids may be too much for traditional PID control techniques to handle. A unique firefly-optimized control approach for frequency stabilization is suggested to solve this problem. This method allows for improved frequency regulation and stability by optimizing PID controller settings using the Firefly algorithm.

The current research investigates the extent to which PI, I and PID controllers, among other conventional control techniques, work to regulate microgrid frequency. The study utilizes the Firefly optimization algorithm to optimize controller parameters, taking advantage of its ability to identify optimal solutions. Additionally, the research evaluates the performance and robustness of Firefly-optimized PID controllers under various load demand scenarios.

The study's findings are anticipated to aid in creating more efficient, resilient, and sustainable Microgrid systems, ultimately enhancing the reliability and sustainability of power supply in remote areas. System assessment, controller design, optimization strategies, and results analysis are all covered in detail in the article.

A critical analysis of the literature survey reveals several research gaps:

- Frequency stabilization in micro-grid systems incorporating solar PV, inverters, and wind turbine generators requires further investigation.
- There is a notable absence of comparative studies examining the effectiveness of traditional regulators (I, PI, PID) within micro-grid systems that incorporate a wide range of components, including Bio-Diesel (BD), Solar Photovoltaic (Solar PV), Electric vehicles (EVs), Diesel Generators (DG), Fuel Cells (FC), Wind Turbines (WTs), Aqua-Electrolysers (AE), and other storage devices.
- The Firefly Algorithm, despite its proven effectiveness in optimization tasks, has not been explored for optimizing controller parameters in Interconnected renewable energy sources in two-area microgrids, like solar photovoltaic systems.

This manuscript addresses these gaps and makes the following key contributions:

- Development of a model for a two-area linked suggested microgrid system with various components, mainly with a Solar PV system for examination of smaller signals.
- Frequency regulation in an interconnected area-linked system with traditional controllers (I, PI, and PID).
- The Firefly Algorithm (FA) optimizes regulatory settings.
- Comparative comparison of classical controllers to discover the most effective.
- Evaluation of the resilience of the FA-tuned PID controller in the presence of fluctuating load requirements and time-constant variations.

2. Components of Proposed Two-Area Interconnected System

2.1. Ship Diesel System

Ship Diesel Generators (SDGs) are preferred as backup power sources in shipboard microgrids due to their rapid startup, high efficiency, and low maintenance requirements. Moreover, SDGs can effectively dampen unstable oscillations in microgrid systems [51]. Equation (1) represents an initial-order function of transmission that may be used to depict the dynamic behavior of an SDG.

$$G_{SDG} = \frac{\mathbf{1}}{(\mathbf{1}+s\boldsymbol{T_{Gs}})(\mathbf{1}+s\boldsymbol{T})} \tag{1}$$

2.2. Electric Vehicles (EV)

Driving, charging, and controlled states are the three main states into which Electric Vehicles (EVs) [60] fall. When an EV is plugged in, it moves from the state of regulation to the state of driving. The capacity of an EV's battery is 3 kW/15 kWh. In the charging condition, which follows a journey, the EV becomes uncontrolled and insensitive to frequency management signals. Electric Vehicles (EVs) in the controlled state vary their State Of Charge (SOC) by dynamically modifying their charging or discharging patterns in response to Frequency Regulation (FR) signals. A probabilistic approach is employed to estimate the typical duration of EV trips and associated energy depletion during unplugged periods to replicate realistic driving patterns.

Controllable electric cars have limited charging and discharging capacities due to their high output (± 3 kW) and energy capacity (80-90%) of the state of charge. Each EV reports its control status to the nearby monitoring center, specifying whether it is controlled-in or plugged-out. The standalone electric vehicle battery's energy behaviour during management is simulated using a mathematical framework. The model below calculates total battery charge or discharge power in the controlled state by taking into consideration characteristics such as the capacity of the inverter (μ_e), time constant (T_e) and ramp power rate limitations (δ_e).The model additionally incorporates the EV battery's maximum and least controlled energy, given by E_{max} and E_{min} respectively.

The charging and discharging power is indicated by ΔP_{Ev}.
Idle mode: $\Delta P_{Ev} = 0$
Discharging mode: $\Delta P_{Ev} > 0$
Charging mode: $\Delta P_{Ev} < 0$.

Electric Vehicles (EVs) can operate within a charging and discharging range of $\pm\mu_e$. However, certain limitations apply. Upon reaching maximum energy capacity (E_{max}), the Electric Vehicle (EV) ceases charging, and discharge is confined to the range of 0 to μ_e. Alternatively, when the stored energy falls below the minimum threshold (E_{min}), The electric vehicle recharges exclusively between an interval of -μ_e to 0. The two factors, K_1 and K_2, are used to establish these energy bounds. The differences among an EV battery's current capacity and its preset limitations are represented by these metrics. In particular, K_1 determines the extra energy beyond ($K_1 = E - E_{max}$), while K_2 determines the electrical energy deficit below E_{min} ($K2 = E - E_{min}$), where E is the electric vehicle battery's current capacity.

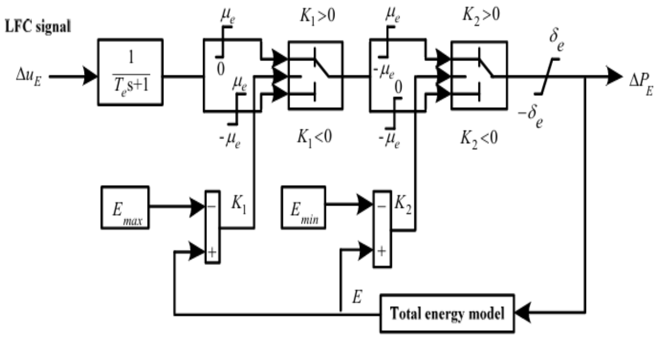

Fig. 1 EV-based concept for a frequency regulating system

The coordinated actions of a sizable fleet of Electric Vehicles (EVs) at a charging location are simulated using a Total Energy Model (TEM). By accounting for the different inverter capabilities of individual EVs, this aggregate model offers a thorough comprehension of their combined dynamics. Ten percent of the total number of EVs in the TEM are thought to be in a controlled condition, meaning they are in the V2G or vehicle-to-grid mode. The model's bidirectional design makes reactive load control possible, allowing the EVs to be linked in series or parallel mode. These EVs obey preset energy capacity restrictions ($E_{\text{control}}^{\text{min}} \leq E_{\text{Control}} \leq E_{\text{control}}^{\text{max}}$) on Load Frequency Control (LFC) signals when charged.

Using the Equations (2) and (3), the energy of controlled electric cars is represented by the symbol Econtrol, with the lowest and highest capacity for energy constraints $E_{\text{control}}^{\text{min}}$ and $E_{\text{control}}^{\text{max}}$, respectively. These limitations ensure an optimal response when faced with frequency regulation signals, which are impacted by the control technique and State Of Charge (SOC). These boundaries are determined by the constantly changing relationship among the command technique and the Status Of Charge (SOC), which produces an optimally attuned response to the regulated frequency signals.

$$E_{\text{control}}^{\text{Min}} = \frac{N_{\text{control}} * C_{\text{kwh}}}{1000} * 0.8 \tag{2}$$

$$E_{\text{control}}^{\text{Max}} = \frac{N_{\text{control}} * C_{\text{kwh}}}{1000} * 0.95 \tag{3}$$

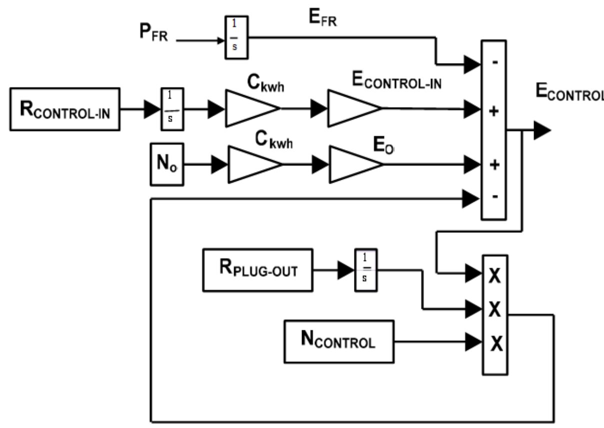

Fig. 2 EV's TEM

All electric cars' combined energy capacity $E_{control}$, may be derived through Equation (4). Four vital energy components-the starting energy condition (E_0), plug-out electrical discharge ($E_{plugout}$), control-in energy inflow ($E_{controlin}$), and the amount of energy allotted for frequency regulation (E_{FR}) are established by this equation.

$$E_{control} = E_{controlin} + E_0 + E_{Plugout} - E_{FR} \tag{4}$$

This case study assumes that eighty percent of electrically powered automobiles are in the control-in condition and twenty percent are in the plugged-out mode. In the Total Energy Model, the cars are initially charged to an energy level of 0.8. The computation of the number of controlled vehicles considers the control-in rate, plug-out rate, and the initial population of controllable vehicles, as depicted in Figure 3.

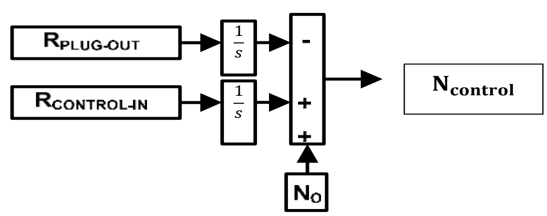

Fig. 3 Pool of controllable electric vehicles

2.3. Diesel Generator

Small-scale Diesel Generator (DG) systems provide numerous advantages, including swift startup, enhanced reliability, and increased energy efficiency. DG systems modulate their power output to maintain frequency stability in response to load demand fluctuations, leveraging fuel control systems [61]. With a linearized transfer function, this fuel regulation mechanism may be statistically expressed in Equation (5).

$$G_{Dg} = \frac{K_T}{\left(1+sT_T\right)} \frac{K_G}{\left(1+sT_G\right)} \tag{5}$$

2.4. Biodiesel Generator

Biodiesel, a bio-derived fuel, is produced through the esterification of organic materials such as sugars, starches, or vegetable oils. As a renewable and eco-friendly energy source, biodiesel offers a sustainable alternative without harming the environment. Equation (6) describes an initial-order function of transfer that may be used to numerically explain the dynamic behavior of a biodiesel-powered generator [62].

$$G_{Dg} = \frac{K_{va}}{(1+sT_{va})}\frac{K_{Be}}{(1+sT_{Be})} \tag{6}$$

2.5. Fuel Cell (FC) and Aqua-Electrolyzer (AE)

An Aqua-Electrolyzer (AE) leverages excess energy from hydrogen gas from a Wind Turbine Generator (WTG), which is then utilized by a Fuel Cell (FC) [63] to generate electricity. The FC produces electrical energy from hydrogen's chemical energy through a combustion-free reaction with air, offering benefits such as minimal environmental impact and high efficiency. Mathematical Equations (7) and (8) give representations of the AE and FC systems.

$$G_{AE} = \frac{K_{AE}}{(1+sT_{AE})} \tag{7}$$

$$G_{FC} = \frac{K_{FC}}{(1+sT_{FC})} \tag{8}$$

2.6. Wind Turbine

Wind Turbine Generators (WTGs) [64] harness renewable energy from wind, with their power output varying directly with wind speed, as mathematically described in Equation (9).

$$G_{wt} = \frac{K_{wt}}{(1+sT_{wt})} \tag{9}$$

2.7. Biogas Plant

The anaerobic decomposition of organic materials produces biogas, a good substitute for traditional generators powered by diesel (DGs). A small-signal transfer function is presented in Equation (10), which can be used to statistically illustrate a BioGas Generator's (BGG) [65] dynamic behavior.

$$G_{Bg} = \frac{K_{bg}(1+sX_C)}{(1+sY_C)(1+sB_b)}\ \frac{(1+sT_{Cr})}{(1+sT_{Bg})}\ \frac{1}{(1+sT_{Bt})} \tag{10}$$

2.8. Storage System

Short-term power fluctuations are common in microgrids, and a Battery Energy Storage System (BESS) helps mitigate these issues [64]. Variations in frequency are kept within reasonable bounds by the BESS's efficient control of these variations. However, because of the time needed for charging, a BESS's reaction time is constrained, usually falling within a few seconds. By dynamically storing energy during non-peak times, a Flywheel Energy Storage System (FESS) enables rapid power distribution throughout times of highest demand. Equations (11) and (12) define the linearized transfer functions that characterize the mathematical representations of these systems.

$$G_{bes} = \frac{K_{bes}}{(1+sT_{bes})} \tag{11}$$

$$G_{Fes} = \frac{K_{Fes}}{(1+sT_{Fes})} \tag{12}$$

2.9. Solar PV System

In solar Photovoltaic (PV) systems, sunlight is captured by panels and transformed into electrical power. The Direct Current (DC) power is subsequently converted to AC power, synced with the grid, and maximized for energy production via tracking of Maximum Power Points (MPPT). This coupling allows smooth functioning inside the microgrid's isolated and grid-connected modes.

$$G_{PV}(s) = \frac{K_{pv}}{1+sT_{pv}} \tag{13}$$

The connection involving the Direct Current (DC) converter's voltage supply and output electrical power is represented by a transfer function commonly used to characterize the inverter's fluctuation efficiency. The response of the inverter may be represented using the following model for dynamic control analysis:

$$G_{inv}(s) = \frac{K_{inv}}{1+sT_{inv}} \tag{14}$$

The transfer function may be used to represent the inverter's output and the interconnection device's reaction to grid circumstances for a first-order approximation [14]:

$$G_{int}(s) = \frac{K_{int}}{1+sT_{int}} \tag{15}$$

The complete solar pv system with inverter and interconnected switch [66], which is added to the proposed Two-Area Interconnected Micro Grid mechanism, can be shown as depicted in Figure 4.

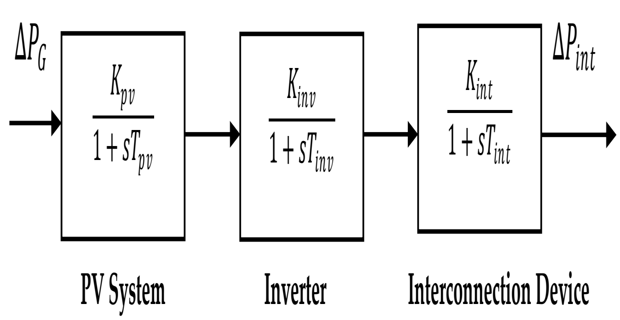

Fig. 4 Inverter and interconnection device for a Solar PV System

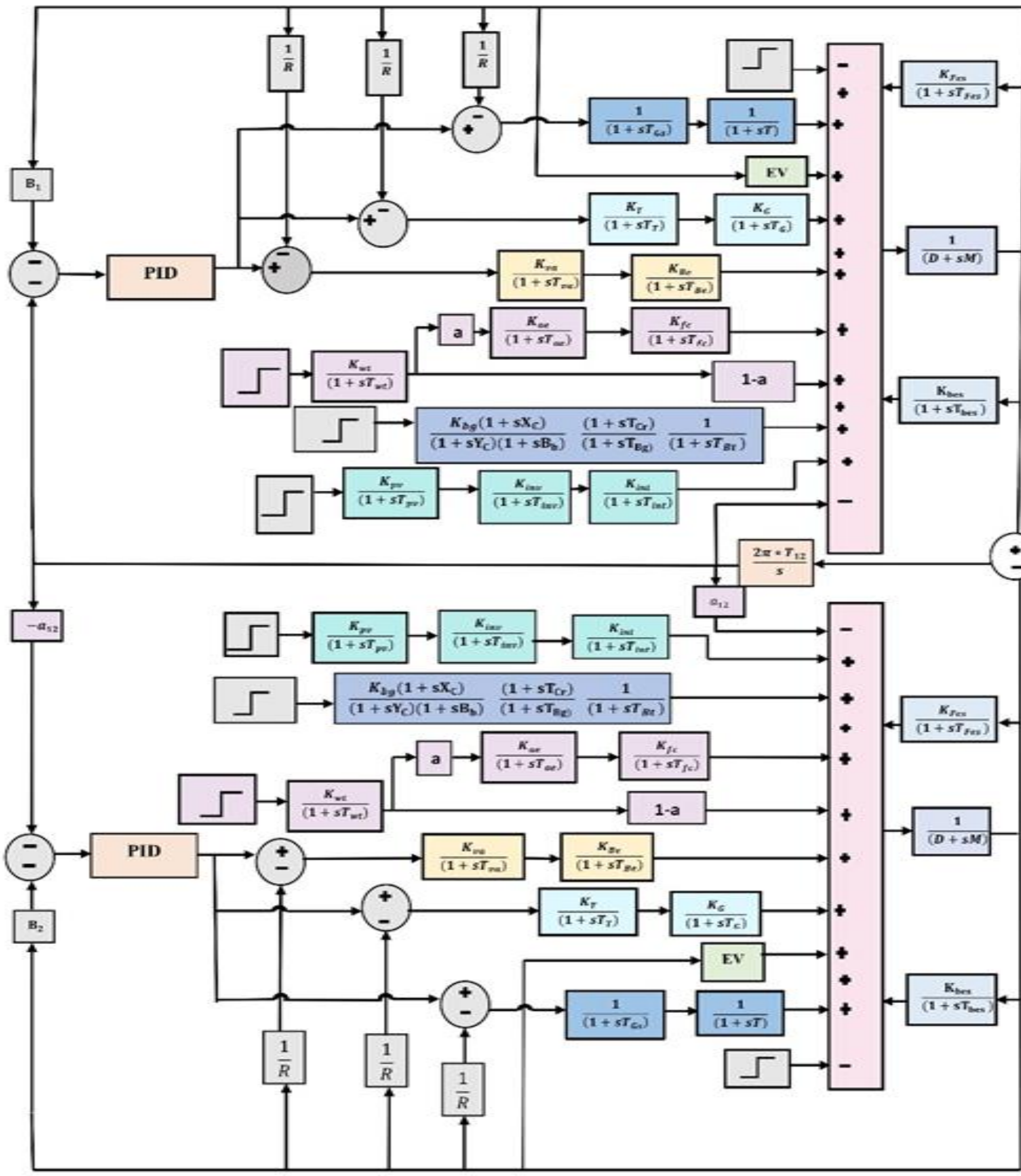

Fig. 5 Schematic representation for the suggested interconnected two-area microgrid configuration

The microgrid setup shown in Figure 5 is thoroughly examined, and several control techniques are used to improve system stability and reduce oscillations. The optimization goal is to minimize the performance index J_{MIN}, as expressed in Equation (16), thereby achieving improved overall system performance.

$$J_{MIN} = \int_0^{Time} \{\Delta f_1^2 + \Delta f_2^2 + \Delta P_{tie}^2\} dt \tag{16}$$

Where Δf_1^2, Δf_2^2, and ΔP_{tie}^2 reflects the squares of the frequency variations in areas 1 and 2 and the twinning power that links them.

3. Implemented Regulators

To address oscillation stabilization, this research employs classical control approaches - specifically Integral (I), Controllers that are Proportional Integral Derivative (PID) and Proportional Integral (PI) are used in both control domains. Adjustable parameters for these controllers are: Kp for P, Ki for I, Ki and Kp for PI, Kp and Kd for PD, Ki, Kp and Kd for PID. A mathematical representation of the PID control mechanism in the temporal domain may be found in the following formula (17).

$$P(t) = Kp\ ACE + Ki \int ACE\ dt + Kd \frac{d}{dt} ACE \tag{17}$$

The Area Control Error (ACE), which represents the overall performance of the system, is a composite statistic that includes both frequency (Δf) and tie-line power exchange (ΔP_{Tie}) variations.

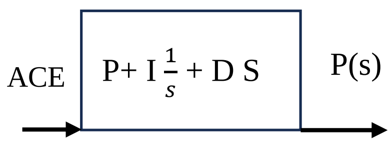

Fig. 6 Mathematical formulation of PID controller

Controllers ensure stability, regulate frequency and manage power flow in a microgrid system with two connecting areas. Three fundamental controller types are employed.

3.1. Integral (I) Controller

This type of controller changes output depending on prior error levels, eliminating steady-state errors but may introduce instabilities.

3.2. Proportional Integral (PI) Controller

In contrast to I controllers, Quick response is provided by the PI controller times and lowers steady-state errors by integrating integral with proportional actions.

3.3. Controller for Proportional Integral Derivatives

The PID controller improves overall stability, minimizes oscillations, and provides the quickest reaction by including derivative control action, which builds upon the PI controller.

3.4. Proportional (P) Controller

In order to control output, a proportional (P) controller scales it in accordance with the present departure from the target value. Because mistakes and control actions are directly related, the controller may react quickly.

3.5. Proportional and Derivative (PD) Controller

A Proportional and Derivative controller blends the control's derivation and proportional action to increase the system's efficiency. In order to facilitate predicted adjustments and avoid overshoot, the derivative term considers the error's rate of change. Certain optimization techniques must be used to modify the parameters to lessen the oscillation magnitudes and settling time. Therefore, this research uses firefly algorithm-tuned regulators for frequency management in the proposed two-area linked microgrid system.

4. The Firefly Algorithm (FA)

The algorithm of fireflies is a naturalistic optimization method that solves challenging problems by simulating fireflies' social behaviour. The occurrence of fireflies employing bioluminescence to attract possible mates serves as the conceptual foundation for the FA. Three main rules form the basis of the algorithm's operation:

4.1. Attraction

Fireflies are drawn to those who are more luminescent, and those who are less dazzling will move to accommodate them.

4.2. Luminescence Intensity

The lack of a brighter firefly makes movement unpredictable.

4.3. Random Movement

The lack of a brighter firefly makes movement unpredictable. Applications of the FA span various domains, including optimization, benchmarking, networking, and image processing.

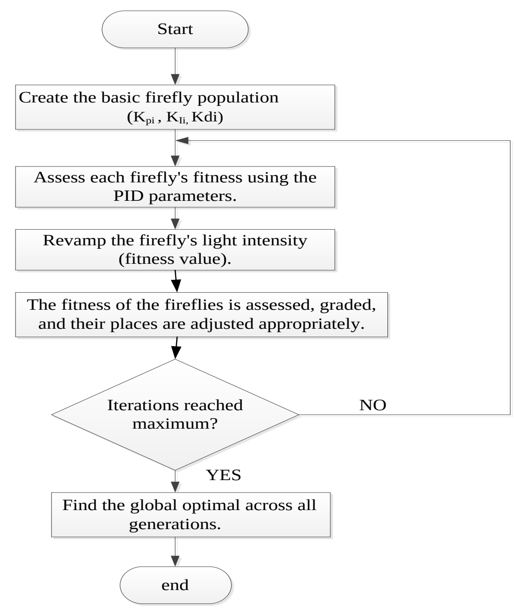

Fig. 7 Flowchart depicting the Firefly Algorithm's workflow

In this context, $\boldsymbol{x}_i$ represents the solution vector or spatial location of firefly i within the search space at iteration q. γ indicates the light absorption coefficient, while β_0 indicates the greatest attraction (when $r_{ij} = 0$). Furthermore, the vector $\in_i^q$ is produced randomly and has a normal distribution, and the scaling factor for the step size is α. The firefly's attraction, denoted by β, is calculated using the formula and decreases as it grows in distance.

$$\beta = \beta_0 e^{-\gamma r_{ij}^2}$$

where β_0 represents the maximum attractiveness at zero distance. The Cartesian distance metric is used to calculate the separation among either of the fireflies positioned at $\boldsymbol{x}_i$ and $\boldsymbol{x}_j$, respectively:

$$\mathbf{r}_{ij} = \| \boldsymbol{x}_i - \boldsymbol{x}_j \| = \sqrt{\sum_{k=1}^{d} (\boldsymbol{x}_{i,k} - \boldsymbol{x}_{j,k})^2}$$

Where $\boldsymbol{x}_{i,k}$ denotes the kth element of the spatial vector $\mathbf{x}_i$ corresponding to the ith firefly. For a two-dimensional scenario, this can be further simplified to:

$$\boldsymbol{r}_{ij} = \sqrt{(\boldsymbol{x}_i - \boldsymbol{x}_j)^2 + (\boldsymbol{y}_i - \boldsymbol{y}_j)^2}$$

In this case, $x_{i,k}$ represents the kth element of the ith firefly's positional value x_i.

Here, like other swarm intelligence techniques such as Bacterial Foraging algorithms, Artificial Bee Colony Optimization and Particle Swarm Optimization (PSO), the Firefly Algorithm (FA) uses collective actions to tackle complicated issues.

5. Result Analysis

5.1. Baseline Conditions

The robustness of a microgrid configuration in Figure 5 to a 2% step nature disruption for both regions is examined in this case study. Traditional actuators (I, PI, and PID) were optimized using the Firefly Technique to lessen this disturbance, yielding the Values of parameters stated in Table 1. Figure 8 illustrates the impact on frequency responses and power in the tie-line. Overshoot/undershoot, settling time and frequency deviation are the key performance measures for frequency stability in interconnected microgrids that assess power quality, stability, and the efficacy of control strategies.

A detailed performance evaluation is presented in Table 2, encompassing metrics such as settling time, peak oscillation amplitude, and minimum oscillation amplitude for each controller.

Table 1. The configurations of the FA-optimized I, PI, and PID control units

Controller/Parameters	I	PI	PID
K_P	-----	1.000	0.9028
K_I	1.00	1.000	0.4947
K_D	------	------	0.3943
K_P	------	0.127	0.9777
K_I	0.1673	0.7761	0.9955
K_D	-------	--------	0.9410

Analysing things in comparison is conducted to assess the convergence properties of these controllers. Figure 9 illustrates their convergence characteristics, revealing that the PID controller exhibits both rapid convergence and the lowest minimum objective function value (J_{min}) among the controllers evaluated. Further validation of this finding is provided through a magnitude analysis presented in Figure 10.

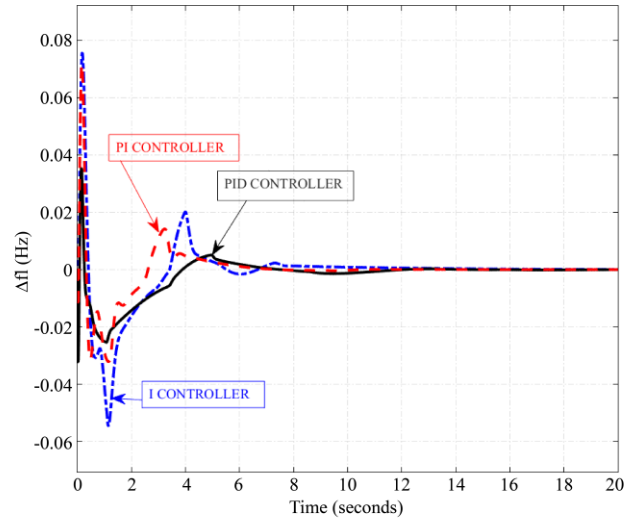

(a) Variation of frequency in Area 1

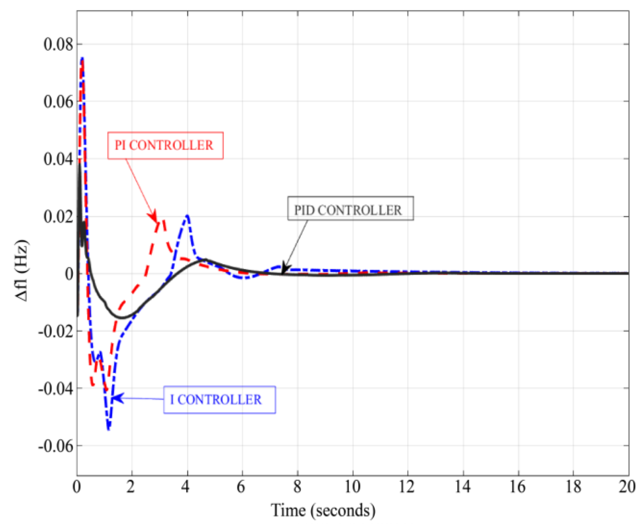

(b) Variation of frequency in Area 2

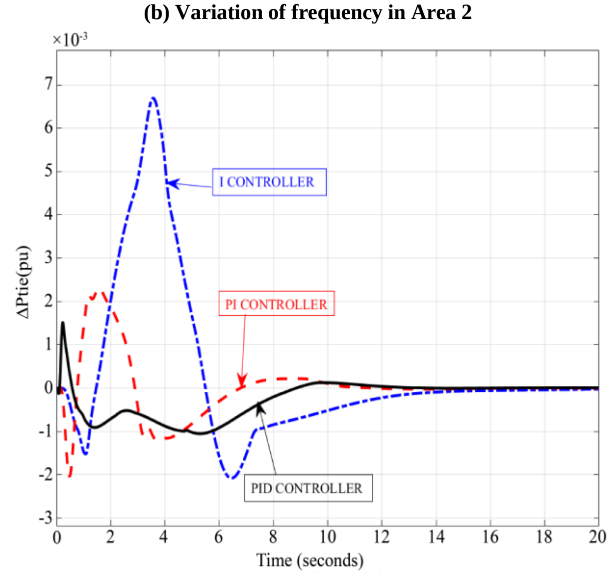

(c) Modifications to power in tie-line

Fig. 8 Dynamics of FA-tuned classical controllers

Table 2. Shows the settling periods and the maximum and minimum magnitudes of the reactions from Figure 8

Duration of Settling									
Dynamic/Response Metrics	**I**	**PI**	**PID**	**I**	**PI**	**PID**	**I**	**PI**	**PID**
Response, Δf_1	15.93	15	15	70.54	71.51	0.3479	40.893	32.04	0.257
Response, Δf_2	15	15	15	75.33	70.49	0,2850	50.44	40.68	0.246
Response, ΔP_{tie}	22.5	22.5	16.675	6.69	2.31	0.7833	2.079	1.993	1.886

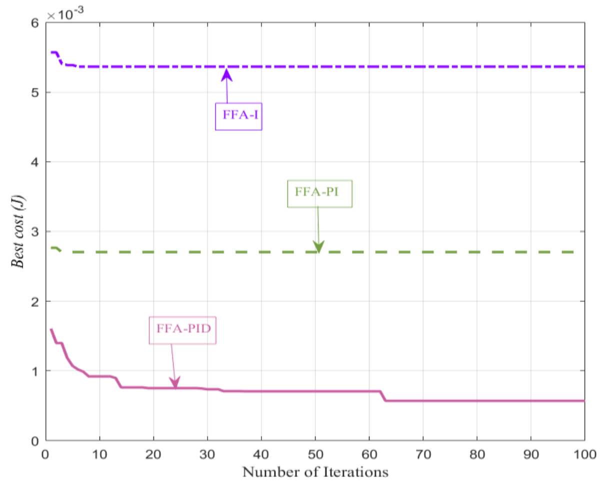

Fig. 9 Convergence of FA-tuned controllers (J_{min} vs Number of iterations)

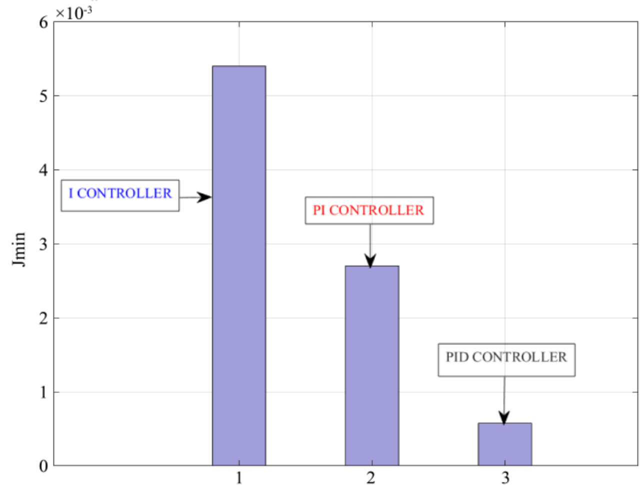

Fig. 10 Magnitude assessment of J_{min} of classical controller

5.2. Smaller and Larger Step Natured Load Disturbance Condition

This investigation assesses the PID controller's insensitivity to greater demands for load in the control regions. A two percent Step-Natured Distortion (SND) is first applied in both regions. In control regions 1 and 2, the SND magnitude is first reduced to 1% and subsequently raised to 3% and 5%, respectively. To assess how well the controller performs in specific situations, the PID parameters (K_p, K_d, and K_i) are adjusted using the Firefly Algorithm (FA). Table 3 displays the values that were obtained.

Table 3. Adjusted Firefly Algorithm settings for 1%, 3%, and 5% step-natured volatility

Controller/Parameters	I	PI	PID
K_P	0.6794	0.9994	0.9764
K_I	0.2957	0.8802	0.9721
K_D	0.9386	0.1308	0.0025
K_P	0.9664	0.4739	0.8783
K_I	0.1514	0.7120	0.8982
K_D	0.9848	0.5391	0.9491

After that, a comparison of the system dynamics is carried out utilizing the returned parameters and the optimal gains listed in Table 4. The outcomes are depicted in Figures 11, 12, and 13.

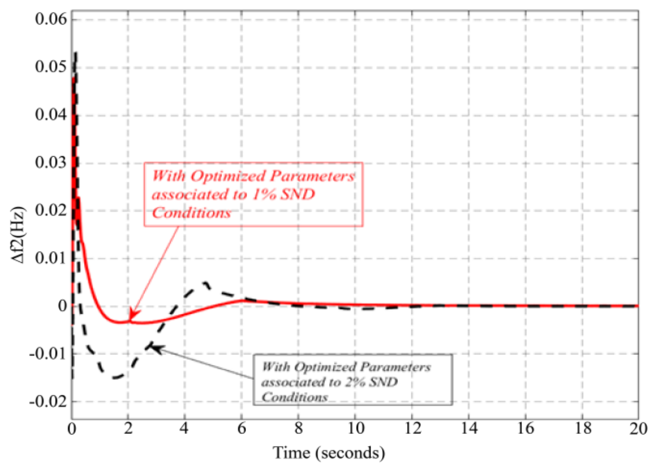

(a) Variation of frequency in area 1

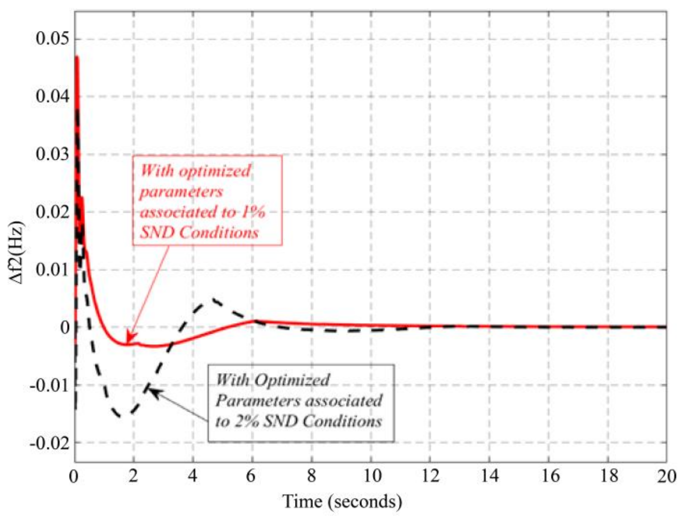

(b) Variation of frequency in area 2

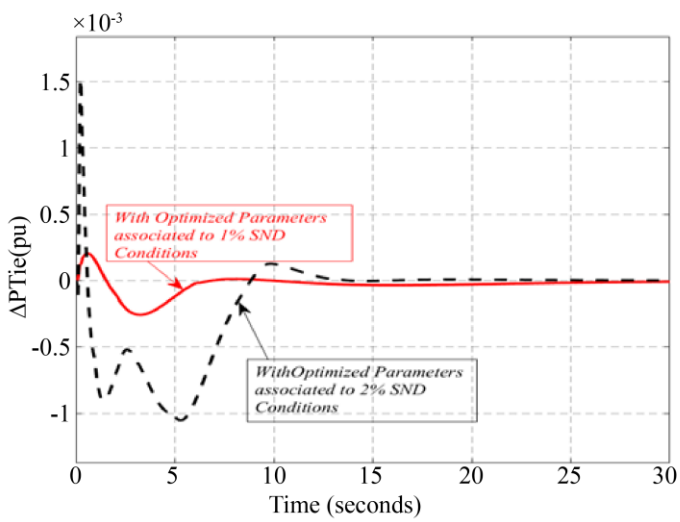

(c) Modifications to power in tie-line

Fig. 11 FA- retuned PID controller dynamics for 1% SND with 2% SND conditions

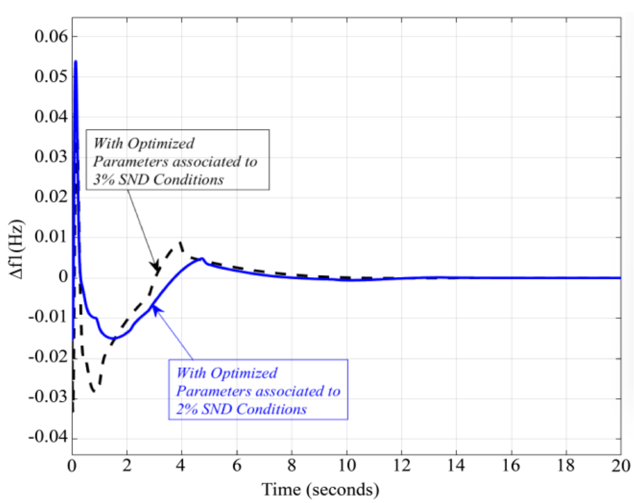

(a) Variation of frequency in area 1

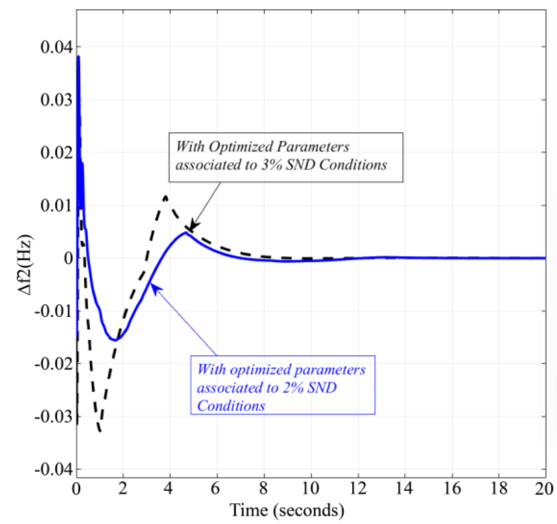

(b) Variation of frequency in area 2

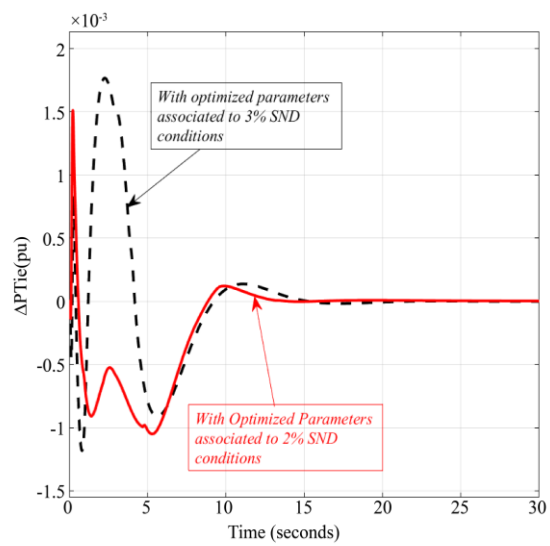

(c) Modifications to power in tie-line

Fig. 12 FA- retuned PID controller dynamics for 3% SND with 2% SND conditions

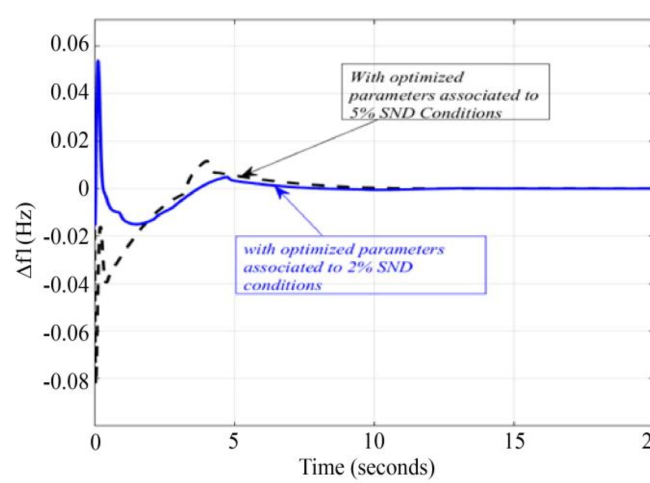

(a) Variation of frequency in area 1

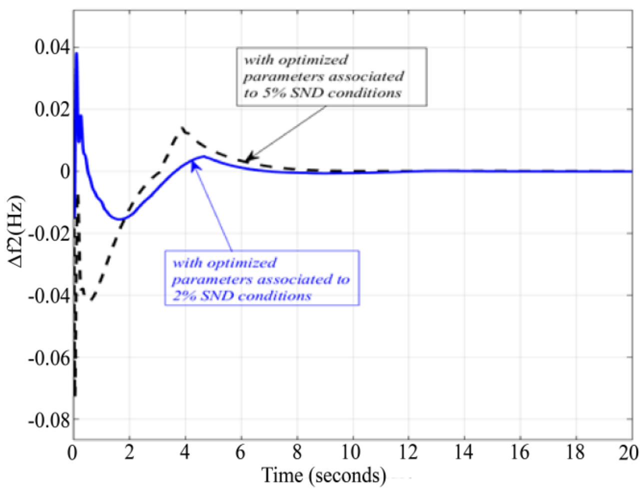

(b) Variation of frequency in area 2

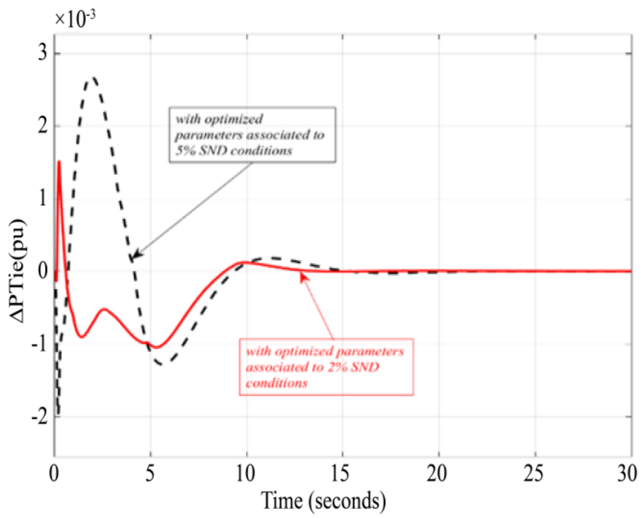

(c) Modifications to power in tie-line

Fig. 13 FA- retuned PID controller dynamics for 5% SND with 2% SND conditions

According to the waveform analysis, the FFA-optimized PID controller in the suggested Interconnected Two-Area Micro Grid setup exhibits faster settling times and reduced oscillation magnitudes for small disturbance amplitudes, outperforming its response under nominal and 2% step disturbance conditions. Moreover, the FFA-tuned PID controller parameters derived under nominal conditions demonstrate robustness, showing minimal sensitivity to larger 3% and 5% disturbance amplitudes.

5.3. Case study for 15,000 Electric Vehicles in Idle Mode and 35,000 Vehicles Under Active Control

Figures 14 (a), (b), and (c) show that as the count of programmable vehicles run by electric power rises, the system's dynamic responsiveness improves, characterized by shorter settling times and diminished frequency and power deviations, compared to scenarios with fewer controllable Electric Vehicles.

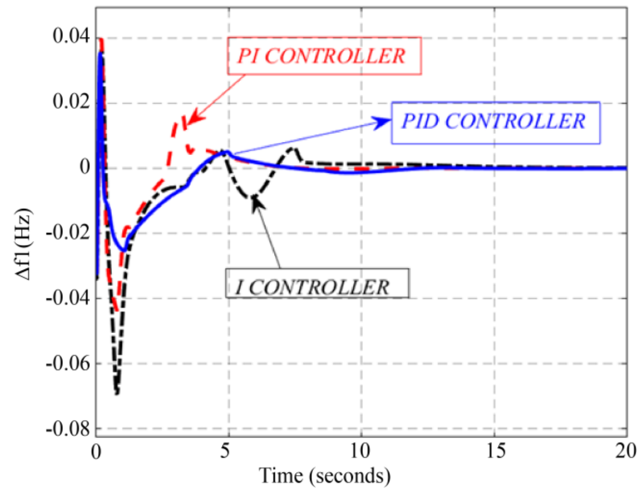

(a) Variation of frequency in area 1

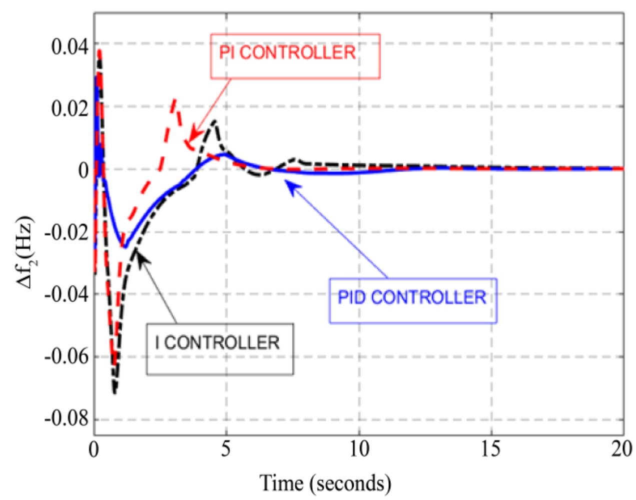

(b) Variation of frequency in area 2

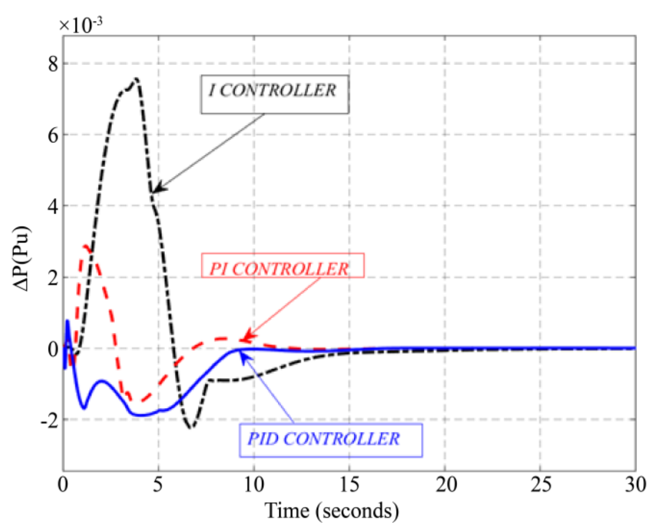

(c) Modifications to power in tie-line

Fig. 14 Dynamics with the reduced number of Electric Vehicles in the Control State

6. Conclusion

The usage of a Proportional Integral Derivative controller is the primary objective of current research. Based on the Firefly Algorithm (FA) to perform frequency restoration in a microgrid system. The interconnected system has two areas and comprises various components, including solar PV systems, an aqua-electrolyzer, a fuel cell, wind turbines, electric vehicles, and energy storage devices. The main conclusions of this system demonstrate how the system of control outperforms the FA-tuned PI and FA-tuned I regulators concerning fluctuation values and settling down times.

In comparing the FA-PID controller to the FA-based I and PI controllers, the latter has the smallest cost parameter value. Additionally, with little variations, the FA-PID controller performs effectively with step-like disruptions. Additionally, the waveforms show that the FA-tuned PID controller settings continue to work well for step-natured disturbances with greater amplitudes. The outcomes demonstrate the FA-PID controller's robustness and proficiency in frequency stabilization applications when subjected to different load disturbances and variations in the number of Electrical Vehicles in the interconnected system subjected to a controllable state. Grid connectivity, electric car charging behaviour, and weather all have an external influence on stabilizing frequency in linked microgrids. Ageing infrastructure and energy storage system performance also affect frequency stability. The investigation of sophisticated optimization methods, coordinated management of dispersed energy supplies, and efficient electric vehicle charging methods are some of the future research areas for frequency stability in interlinked microgrids.

References

[1] Deepesh Sharma, "Load Frequency Control: A Literature Review," *International Journal of Scientific and Technology Research*, vol. 9, no. 2, pp. 6421-6437, 2020. [Google Scholar] [Publisher Link]

[2] Rijo Rajan et al., "Primary Frequency Control Techniques for Large-Scale PV-Integrated Power Systems: A Review," *Renewable and Sustainable Energy Reviews*, vol. 144, 2021. [CrossRef] [Google Scholar] [Publisher Link]

[3] Kanendra Naidu et al., "Performance Investigation of ABC Algorithm in Multi-Area Power System with Multiple Interconnected Generators," *Applied Soft Computing*, vol. 57, pp. 436-451, 2017. [CrossRef] [Google Scholar] [Publisher Link]

[4] Chunyu Chen et al., "Tie-Line Bias Control Applicability to Load Frequency Control for Multi-Area Interconnected Power Systems of Complex Topology," *Energies*, vol. 10, no. 1, 2017. [CrossRef] [Google Scholar] [Publisher Link]

[5] Jing Ma et al., "Research on the Impact of DFIG Virtual Inertia Control on Power System Small-Signal Stability Considering the Phase-Locked Loop," *IEEE Transactions on Power Systems*, vol. 32, no. 3, pp. 2094-2105, 2016. [CrossRef] [Google Scholar] [Publisher Link]

[6] Yi Zhang et al., "Distributed Model Predictive Load Frequency Control of Multi-Area Power System with DFIGS," *IEEE/CAA Journal of Automatica Sinica*, vol. 4, no. 1, pp. 125-135, 2017. [CrossRef] [Google Scholar] [Publisher Link]

[7] Mohammad Hassan Khooban et al., "A New Load Frequency Control Strategy for Micro-Grids with Considering Electrical Vehicles," *Electric Power Systems Research*, vol. 143, pp. 585-598, 2017. [CrossRef] [Google Scholar] [Publisher Link]

[8] Ima O. Essiet, Yanxia Sun, and Zenghui Wang, "Optimized Energy Consumption Model for Smart Home using Improved Differential Evolution Algorithm," *Energy*, vol. 172, pp. 354-365, 2019. [CrossRef] [Google Scholar] [Publisher Link]

[9] Mercedes Ruiz-Cortés et al., "Optimal Charge/Discharge Scheduling of Batteries in Microgrids of Prosumers," *IEEE Transactions on Energy Conversion*, vol. 34, no. 1, pp. 468-477, 2018. [CrossRef] [Google Scholar] [Publisher Link]

[10] Abbas Ketabi, and Masoud Hajiakbari Fini, "An Underfrequency Load Shedding Scheme for Islanded Microgrids," *International Journal of Electrical Power & Energy Systems*, vol. 62, pp. 599-607, 2014. [CrossRef] [Google Scholar] [Publisher Link]

[11] Wenyun Ju, Kai Sun, and Junjian Qi, "Multi-Layer Interaction Graph for Analysis and Mitigation of Cascading Outages," *IEEE Journal on Emerging and Selected Topics in Circuits and Systems*, vol. 7, no. 2, pp. 239-249, 2017. [CrossRef] [Google Scholar] [Publisher Link]

[12] Hassan Bevrani et al., "Power System Frequency Control: an Updated Review of Current Solutions and New Challenges," *Electric Power Systems Research*, vol. 194, 2021. [CrossRef] [Google Scholar] [Publisher Link]

[13] Hassan Bevrani, *Robust Power System Frequency Control*, Springer International Publishing, 2nd ed., 2009. [Publisher Link]

[14] Katsuhiko Ogata, *Modern Control Engineering*, 5th ed., Prentice Hall, 2009. [Publisher Link]

[15] K. Naidu, H. Mokhlis, and A.H.A. Bakar, "Multi Objective Optimization using Weighted Sum Artificial Bee Colony Algorithm for Load Frequency Control," *International Journal of Electrical Power & Energy Systems*, vol. 55, pp. 657-667, 2014. [CrossRef] [Google Scholar] [Publisher Link]

[16] Mohamed Khamies et al., "A Robust Pid Controller based on Linear Quadratic Gaussian Approach for Improving Frequency Stability of Power Systems Considering Renewables," *ISA Transactions*, vol. 117, pp. 118-138, 2021. [CrossRef] [Google Scholar] [Publisher Link]

[17] Abhineet Prakash, Kundan Kumar, and Sanjoy Kumar Parida, "PIDF (1+ FOD) Controller for Load Frequency Control with SSSC and AC–DC Tie-Line in Deregulated Environment," *IET Generation, Transmission and Distribution*, vol. 14, no. 14, pp. 2751-2762, 2020. [CrossRef] [Google Scholar] [Publisher Link]

[18] L. Hongyue, Xihuai Wang, and Jianmei Xiao, "Adaptive Event-Triggered Load Frequency Control for Interconnected Microgrids by Observer-Based Sliding Mode Control," *IEEE Access*, vol. 7, pp. 68271-68280, 2019. [CrossRef] [Google Scholar] [Publisher Link]

[19] Satish Kumar Ramoji, and Lalit Chandra Saikia, "Maiden Application of Fuzzy-2DOFTID Controller in Unified Voltage-Frequency Control of Power System," *IETE Journal of Research*, vol. 69, no. 7, pp. 4738-4759, 2023. [CrossRef] [Google Scholar] [Publisher Link]

[20] Tarkeshwar Mahto et al., "Renewable Generation-Based Hybrid Power System Control using Fractional Order-Fuzzy Controller," *Energy Reports*, vol. 7, pp. 641-653, 2021. [CrossRef] [Google Scholar] [Publisher Link]

[21] Yajian Zhang, and Ting Yang, "Decentralized Switching Control Strategy for Load Frequency Control in Multi-Area Power Systems with Time Delay and Packet Losses," *IEEE Access*, vol. 8, pp. 15838-15850, 2020. [CrossRef] [Google Scholar] [Publisher Link]

[22] Kamlesh Bharti, Vijay P. Singh, and S.P. Singh, "C *IETE Journal of Research*, vol. 68, no. 4, pp. 2433-2444, 2022. [CrossRef] [Google Scholar] [Publisher Link]

[23] Yasser Ahmed Dahab, Hussein Abubakr, and Tarek Hassan Mohamed, "Adaptive Load Frequency Control of Power Systems Using Electro-Search Optimization Supported by the Balloon Effect," *IEEE Access*, vol. 8, pp. 7408-7422, 2020. [CrossRef] [Google Scholar] [Publisher Link]

[24] Pegah Ojaghi, and Mehdi Rahmani, "Lmi-Based Robust Predictive Load Frequency Control for Power Systems with Communication Delays," *IEEE Transactions on Power Systems*, vol. 32, no. 5, pp. 4091-4100, 2017. [CrossRef] [Google Scholar] [Publisher Link]

[25] Xiaoshuang Chen et al., "Optimal Control of AGC Systems Considering Non-Gaussian Wind Power Uncertainty," *IEEE Transactions on Power Systems*, vol. 34, no. 4, pp. 2730-2743, 2019. [CrossRef] [Google Scholar] [Publisher Link]

[26] Ragini Patel et al., "Enhancing Optimal Automatic Generation Control in a Multi-Area Power System with Diverse Energy Resources," *IEEE Transactions on Power Systems*, vol. 34, no. 5, pp. 3465-3475, 2019. [CrossRef] [Google Scholar] [Publisher Link]

[27] Zonggen Yi et al., "A Highly Efficient Control Framework for Centralized Residential Charging Coordination of Large Electric Vehicle Populations," *International Journal of Electrical Power and Energy Systems*, vol. 117, 2020. [CrossRef] [Google Scholar] [Publisher Link]

[28] Severin Nowak, Liwei Wang, and Malcolm S. Metcalfe, "Two-Level Centralized and Local Voltage Control in Distribution Systems Mitigating Effects of Highly Intermittent Renewable Generation," *International Journal of Electrical Power and Energy Systems*, vol. 119, 2020. [CrossRef] [Google Scholar] [Publisher Link]

[29] Hossam Hassan Ali et al., "Multi-Verse Optimizer for Model Predictive Load Frequency Control of Hybrid Multi-Interconnected Plants Comprising Renewable Energy," *IEEE Access*, vol. 8, pp. 114623-114642, 2020. [CrossRef] [Google Scholar] [Publisher Link]

[30] M. Elsisi et al., "Optimal Design of Model Predictive Control with Superconducting Magnetic Energy Storage for Load Frequency Control of Nonlinear Hydrothermal Power System Using Bat Inspired Algorithm," *Journal of Energy Storage*, vol. 12, pp. 311-318, 2017. [CrossRef] [Google Scholar] [Publisher Link]

[31] Hazem F. Feshara et al., "Performance Evaluation of Variable Structure Controller Based on Sliding Mode Technique for a Grid-Connected Solar Network," *IEEE Access*, vol. 7, pp. 84349-84359, 2019. [CrossRef] [Google Scholar] [Publisher Link]

[32] Satish Kumar, and Ashwani Kumar, "Design and Optimization of Multiple Facts Devices for Congestion Mitigation using Sensitivity Factor with Wind Integrated System," *IETE Journal of Research*, vol. 68, no. 6, pp. 4085-4099, 2022. [CrossRef] [Google Scholar] [Publisher Link]

[33] Ban H. Alajrash et al., "A Comprehensive Review of Facts Devices in Modern Power Systems: Addressing Power Quality, Optimal Placement, and Stability with Renewable Energy Penetration," *Energy Reports*, vol. 11, pp. 5350-5371, 2024. [CrossRef] [Google Scholar] [Publisher Link]

[34] Abdul Latif et al., "A Review on Fractional Order (Fo) Controllers' Optimization for Load Frequency Stabilization in Power Network," *Energy Report*, vol. 7, pp. 4009-4021, 2021. [CrossRef] [Google Scholar] [Publisher Link]

[35] Mandeep Sharma, Surya Prakash, and Sahaj Saxena, "Robust Load Frequency Control Using Fractional-Order Tid-Pd Approach Via Salp Swarm Algorithm," *IETE Journal of Research*, vol. 69, no. 5, pp. 2710-2726, 2023. [CrossRef] [Google Scholar] [Publisher Link]

[36] Haitham S. Ramadan, Ahmed Fathy, and Mohamed Becherif, "Optimal Gain Scheduling of VSC-HVDC System Sliding Mode Control Via Artificial Bee Colony and Mine Blast Algorithms," *IET Generation, Transmission and Distribution*, vol. 12, no. 3, pp. 661-669, 2018. [CrossRef] [Google Scholar] [Publisher Link]

[37] Kai Ma et al., "Resource Allocation for Smart Grid Communication Based on a Multi-Swarm Artificial Bee Colony Algorithm with Cooperative Learning," *Engineering Applications of Artificial Intelligence*, vol. 81, pp. 29-31, 2019. [CrossRef] [Google Scholar] [Publisher Link]

[38] Akhilesh Panwar, Gulshan Sharma, and Ramesh C. Bansal, "Optimal AGC Design for a Hybrid Power System Using Hybrid Bacteria Foraging Optimization Algorithm," *Electric Power Components and Systems*, vol. 47, no. 11-12, pp. 955-965, 2019. [CrossRef] [Google Scholar] [Publisher Link]

[39] Ben Niu et al., "Cooperative Bacterial Foraging Optimization Method for Multi-Objective Multi-Echelon Supply Chain Optimization Problem," *Swarm and Evolutionary Computation*, vol. 49, pp. 87-101, 2019. [CrossRef] [Google Scholar] [Publisher Link]

[40] Puja Dash, Lalit Chandra Saikia, and Nidul Sinha, "Automatic Generation Control of Multi Area Thermal System Using Bat Algorithm Optimized PD-PID Cascade Controller," *International Journal of Electrical Power & Energy Systems*, vol. 68, pp. 364-372, 2015. [CrossRef] [Google Scholar] [Publisher Link]

[41] H. Shayeghi, H.A. Shayanfar, and A. Jalili, “Multi-Stage Fuzzy Pid Power System Frequency Control,” *Energy Conversion and Management*, vol. 49, no. 18-19, pp. 2829-2845, 2006. [CrossRef] [Google Scholar] [Publisher Link]

[42] S. Surender Reddy, “Bat Algorithm-Based Back Propagation Approach for Short-Term Load Forecasting Considering Weather Factors,” *Electrical Engineering*, vol. 100, no. 3, pp. 1297-1303, 2018. [CrossRef] [Google Scholar] [Publisher Link]

[43] Hassan Y. Mahmoud et al., “Hybrid Cuckoo Search Algorithm and Grey Wolf Optimiser-Based Optimal Control Strategy for Performance Enhancement of HVDC-Based Offshore Wind Farms,” *IET Generation, Transmission and Distribution*, vol. 14, no. 10, pp. 1902-1911, 2020. [CrossRef] [Google Scholar] [Publisher Link]

[44] Teimour Hosseinalizadeh et al., “Improvement of Identification Procedure using Hybrid Cuckoo Search Algorithm for Turbine-Governor and Excitation System,” *IEEE Transactions on Energy Conversion*, vol. 34, no. 2, pp. 585-593, 2018. [CrossRef] [Google Scholar] [Publisher Link]

[45] Mandeep Sharma et al., “Optimal Fractional-Order Tilted-Integral-Derivative Controller for Frequency Stabilization in Hybrid Power System using Salp Swarm Algorithm,” *Electric Power Components and Systems*, vol. 48, no. 18, pp. 1912-1931, 2021. [CrossRef] [Google Scholar] [Publisher Link]

[46] Banaja Mohanty, Sidhartha Panda, and P.K. Hota, “Controller Parameters Tuning of Differential Evolution Algorithm and its Application to Load Frequency Control of Multi-Source Power System,” *International Journal of Electrical Power and Energy Systems*, vol. 54, pp. 77-85, 2014. [CrossRef] [Google Scholar] [Publisher Link]

[47] Aeidapu Mahesh, and Kanwarjit Singh Sandhu, “A Genetic Algorithm Based Improved Optimal Sizing Strategy for Solar-Wind-Battery Hybrid System using Energy Filter Algorithm,” *Frontiers in Energy*, vol. 14, pp. 139-151, 2020. [CrossRef] [Google Scholar] [Publisher Link]

[48] Haseena Kuttomparambil Abdulkhader, Jeevamma Jacob, and Abraham T. Mathew, “Fractional-Order Lead-Lag Compensator-Based Multi-Band Power System Stabiliser Design using a Hybrid Dynamic Ga-Pso Algorithm,” *IET Generation, Transmission and Distribution*, vol. 12, no. 13, pp. 3248-3260, 2018. [CrossRef] [Google Scholar] [Publisher Link]

[49] Nour EL Yakine Kouba et al., “A New Optimal Load Frequency Control Based on Hybrid Genetic Algorithm and Particle Swarm Optimization,” *International Journal on Electrical Engineering and Informatics*, vol. 9, no. 3, pp. 418-440, 2017. [Google Scholar] [Publisher Link]

[50] Nandala Nagarjuna, and G. Shankar, “Load Frequency Control of Two Area Power System with AC-DC Tie Line Using PSO Optimized Controller,” *International Conference on Power and Advanced Control Engineering*, Bengaluru, India, pp. 227-231, 2015. [CrossRef] [Google Scholar] [Publisher Link]

[51] Utkarsh Raj, and Ravi Shankar, “Deregulated Automatic Generation Control Using Novel Opposition-Based Interactive Search Algorithm Cascade Controller Including Distributed Generation and Electric Vehicle,” *Iranian Journal of Science and Technology, Transactions of Electrical Engineering*, vol. 44, pp. 1233-1251, 2020. [CrossRef] [Google Scholar] [Publisher Link]

[52] Somnath Ganguly, Chandan Kumar Shiva, and V. Mukherjee, “Frequency Stabilization of Isolated and Grid Connected Hybrid Power System Models,” *Journal of Energy Storage*, vol. 19, pp. 145-159, 2018. [CrossRef] [Google Scholar] [Publisher Link]

[53] Sandhya Kumari, and Gauri Shankar, “Maiden Application of Cascade Tilt-Integral-Derivative Controller in Load Frequency Control of Deregulated Power System,” *International Transactions on Electrical Energy Systems*, vol. 30, no. 3, 2020. [CrossRef] [Google Scholar] [Publisher Link]

[54] Anouar Farah et al., “A Novel Chaotic Teaching-Learning-Based Optimization Algorithm for Multi-Machine Power System Stabilizers Design Problem,” *International Journal of Electrical Power and Energy Systems*, vol. 77, pp. 197-209, 2016. [CrossRef] [Google Scholar] [Publisher Link]

[55] Prakash K. Ray et al., “A Hybrid Firefly-Swarm Optimized Fractional Order Interval Type-2 Fuzzy PID-PSS for Transient Stability Improvement,” *IEEE Transactions on Industry Applications*, vol. 55, no. 6, pp. 6486-6498, 2019. [CrossRef] [Google Scholar] [Publisher Link]

[56] S.M. Abd-Elazim, and E.S. Ali, “Firefly Algorithm-Based Load Frequency Controller Design of a Two-Area System Composing of PV Grid and Thermal Generator,” *Electrical Engineering*, vol. 100, pp. 1253-1262, 2018. [CrossRef] [Google Scholar] [Publisher Link]

[57] Mohammad-Hassan Khooban et al., “Shipboard Microgrids: A Novel Approach to Load Frequency Control,” *IEEE Transactions on Sustainable Energy*, vol. 9, no. 2, pp. 843-852, 2017. [CrossRef] [Google Scholar] [Publisher Link]

[58] Shreya Vishnoi et al., “Frequency Stabilization in an Interconnected Micro-Grid using Smell Agent Optimization Algorithm-Tuned Classical Controllers Considering Electric Vehicles and Wind Turbines,” *Energies*, vol. 16, no. 6, 2023. [CrossRef] [Google Scholar] [Publisher Link]

[59] Xin-She Yang, “Firefly Algorithm, Stochastic Test Functions and Design Optimisation,” *International Journal of Bio-Inspired Computation*, vol. 2, no. 2, pp. 78-84, 2010. [CrossRef] [Google Scholar] [Publisher Link]

[60] Koichiro Shimizu et al., “Load Frequency Control in Power System Using Vehicle-to-Grid System Considering the Customer Convenience of Electric Vehicles,” *International Conference on Power System Technology*, Zhejiang, China, 2010. [CrossRef] [Google Scholar] [Publisher Link]

[61] Jun Yang et al., “Load Frequency Control in Isolated Micro-Grids with Electrical Vehicles Based on Multivariable Generalized Predictive Theory,” *Energies*, vol. 8, no. 3, pp. 2145-2164, 2015. [CrossRef] [Google Scholar] [Publisher Link]
[62] Mausri Bhuyan, Amar Kumar Barik, and Dulal Chandra Das, “Goa Optimized Frequency Control of Solar-Thermal/Sea-Wave/Biodiesel Generator Based Interconnected Hybrid Microgrids with Dc Link,” *International Journal of Sustainable Energy*, vol. 39, no. 7, pp. 615-633, 2020. [CrossRef] [Google Scholar] [Publisher Link]
[63] Shashi Kant Pandey et al., “Frequency Regulation in Hybrid Power Systems using Particle Swarm Optimization and Linear Matrix Inequalities Based Robust Controller Design,” *International Journal of Electrical Power & Energy Systems*, vol. 63, pp. 887-900, 2014. [CrossRef] [Google Scholar] [Publisher Link]
[64] Dong-Jing Lee, and Li Wang, “Small-Signal Stability Analysis of an Autonomous Hybrid Renewable Energy Power Generation/Energy Storage System Part I: Time-Domain Simulations,” *IEEE Transactions on Energy Conversion*, vol. 23, no. 1, pp. 311-320, 2008. [CrossRef] [Google Scholar] [Publisher Link]
[65] H. Shayeghi, A. Rahnama, and H.H. Alhelou, “Frequency Control of Fully-Renewable Interconnected Microgrid using Fuzzy Cascade Controller with Demand Response Program Considering,” *Energy Reports*, vol. 7, pp. 6077-6094, 2021. [CrossRef] [Google Scholar] [Publisher Link]
[66] Bevrani, Hassan et al., “Intelligent Frequency Control in an Ac Microgrid: Online Pso-Based Fuzzy Tuning Approach,” *IEEE Transactions on Smart Grid*, vol. 3, no. 4, pp. 1935-1944, 2012. [CrossRef] [Google Scholar] [Publisher Link]

Appendix

Table 4. System parametric values and nomenclature

Representations	Details	Mathematical Values
T_{Gs}, T, and R_s	Temporal factors and regulator settings of the ship diesel generators	0.5, 0.25, 3
K_G, K_T, T_T, T_G, and R	Gains, time constraints, and governor metrics of diesel generator	1, 1, 0.1 sec, 8 sec, 2.5
K_{va}, K_{Be}, T_{va}, T_{Be}, and R	Gains, time constraints, and governor metrics of bio-diesel generator	1, 1, 0.05 sec, 0.5 sec, 2.4
Yc, K_{bg}, X_c T_{Bt} T_{cr}, and T_{Bg}	Bio-gas turbine’s Gain, reactance, admittance, and time constraints metrics	0.5, 0.6, 1, 0.05, 0.01 s, 0.23 s, 0.2 s
T_{ae} and K_{ae}	Aqua-electrolyzer’s Time Constraint and Gain	1/500, 0.5 s
T_{fc} and K_{fc}	Fuel cell’s time constraint and Gain	1/100, 4 s
Tbes and Kbes	Battery energy storage’s Time constraint and Gain	−1/300, 0.1 s
KFes and TFes	FESS gain and time constraints	−1/100, 0.1 s
T12	Synchronizing power co-efficient	0.0867s
Δ	Change	-------
T_{pv} and K_{pv}	Photo Voltaic system’s time and Gain constraints	1.8s,1
T_{inv} and K_{inv}	Inverter time constant and Gain constant	0.04,1
T_{inc} and K_{inc}	Time constant and Gain Interconnected system	0.004,1